Spectrochimica Acta Part A: Molecular and Biomolecular Spectroscopy 107 (2013) 241–247

Contents lists available at SciVerse ScienceDirect

Spectrochimica Acta Part A: Molecular and Biomolecular Spectroscopy

journal homepage: www.elsevier.com/locate/saa

Vibrational spectroscopy of the phosphate mineral lazulite – (Mg, Fe)$Al_2(PO_4)_2{\cdot}(OH)_2$ found in the Minas Gerais, Brazil

Ray L. Frost [a,*], Yunfei Xi [a], Martina Beganovic [b], Fernanda Maria Belotti [c], Ricardo Scholz [b]

[a] School of Chemistry, Physics and Mechanical Engineering, Science and Engineering Faculty, Queensland University of Technology, GPO Box 2434, Brisbane, Queensland 4001, Australia
[b] Geology Department, School of Mines, Federal University of Ouro Preto, Campus Morro do Cruzeiro, Ouro Preto, MG 35400-00, Brazil
[c] Federal University of Itajubá, Campus Itabira, Itabira, MG 35903-087, Brazil

HIGHLIGHTS

- In this work, we have studied the structure of lazulite.
- Lazulite is pegmatite phosphate with calculated formula $(Fe_{0.11})Al_{1.86}(PO_4)_{2.08}(OH)_{2.04}$.
- The structure of lazulite was assessed using a combination of Raman and infrared spectroscopy.

GRAPHICAL ABSTRACT

ARTICLE INFO

Article history:
Received 20 September 2012
Received in revised form 6 November 2012
Accepted 23 January 2013
Available online 1 February 2013

Keywords:
Raman spectroscopy
Lazulite
Infrared spectroscopy
Phosphate
Pegmatite

ABSTRACT

This research was done on lazulite samples from the Gentil mine, a lithium bearing pegmatite located in the municipality of Mendes Pimentel, Minas Gerais, Brazil. Chemical analysis was carried out by electron microprobe analysis and indicated a magnesium rich phase with partial substitution of iron. Traces of Ca and Mn, (which partially replaced Mg) were found. The calculated chemical formula of the studied sample is: $(Mg_{0.88}, Fe_{0.11})Al_{1.87}(PO_4)_{2.08}(OH)_{2.02}$. The Raman spectrum of lazulite is dominated by an intense sharp band at 1060 cm^{-1} assigned to PO stretching vibrations of of tetrahedral [PO4] clusters presents into the HPO_4^{2-} units. Two Raman bands at 1102 and 1137 cm^{-1} are attributed to both the HOP and PO antisymmetric stretching vibrations. The two infrared bands at 997 and 1007 cm^{-1} are attributed to the v_1 PO_4^{3-} symmetric stretching modes. The intense bands at 1035, 1054, 1081, 1118 and 1154 cm^{-1} are assigned to the v_3 PO_4^{3-} antisymmetric stretching modes from both the HOP and tetrahedral [PO4] clusters. A set of Raman bands at 605, 613, 633 and 648 cm^{-1} are assigned to the v_4 out of plane bending modes of the PO_4, HPO_4 and H_2PO_4 units. Raman bands observed at 414, 425, 460, and 479 cm^{-1} are attributed to the v_2 tetrahedral PO_4 clusters, HPO_4 and H_2PO_4 bending modes. The intense Raman band at 3402 and the infrared band at 3403 cm^{-1} are assigned to the stretching vibration of the OH units. A combination of Raman and infrared spectroscopy enabled aspects of the molecular structure of the mineral lazulite to be understood.

Introduction

The minerals of lazulite group are basic hydro-phosphates and arsenates with the general chemical composition $M_1^2 + M_2^{3+}(XO_4)2(OH)_2$, where M_1 can be occupied by Fe^{2+}, Mg, Cu and Zn, and M_2 can be occupied by Al and Fe^{3+}. In the anionic group, X can be occupied by P and As [1]. They crystallize in the monoclinic crystal system, space group $P2_1/c$, and unit cell parameters $a = 7.1526$ Å, $b = 7.278$ Å, $c = 7.2334$ Å, $Z = 2$ and $\beta = 89.233°$ [2]. The name lazulite is used for a solid solution between the end-members lazulite – $MgAl_2(PO_4)_2(OH)_2$ and scorzalite – $FeAl_2(PO_4)_2(OH)_2$ [3]. The mineral is

* Corresponding author. Tel.: +61 7 3138 2407; fax: +61 7 3138 1804.
E-mail address: r.frost@qut.edu.au (R.L. Frost).

1386-1425/$ - see front matter © 2013 Elsevier B.V. All rights reserved.
http://dx.doi.org/10.1016/j.saa.2013.01.056

known since 18th century, and the name lazulite was first used by Klaproth [4]. The mineral is a bright blue color as shown in the Supplementary information as Fig. S1. The color of the mineral is related to the actual composition of the lazulite sample. Other phosphate members of lazulite group are Barbosalite $Fe^{2+}(Fe^{3+})_2^+(PO_4)2(OH)_2$ [2] and Hentschelite – $Cu^{2+}(Fe^{3+})_2 + (PO_4)_2(OH)_2$ [5]. Wet chemical analysis suggested for natural lazulite–scorzalite samples a complete solid-solution series between the end-members [3]. Contrasting results have exclusively been reported by Duggan et al. [6] who proposed a miscibility gap between 35 and 75 mol% scorzalite [7].

Cationic distribution in the lazulite type minerals according to the ideal formula $M^{2+}M_2^{3+}(PO_4)_2(OH)_2$ of lazulite group members leads to the structure type that can be regarded as to be built up of infinite chains of face – sharing oxygen octahedra which are interconnected via PO^{4-} tetrahedra and common hydroxyl ions. The symmetrically equivalent chains run into the [1 1 0] and [−1 1 0] direction (space group $P2_1/c$). The cations occupy three adjacent octahedra forming a trimer denoted as h-cluster [8,9]. Lazulite and scorzalite occur in many regions throughout the world. The main geological environments are related to metamorphic rocks from green schist to amphibolite facies [10–16] and associated to granitic pegmatites [6,17–19]. The mineral is known from quite a wide variety of locations [6,16,17,19–24].

Nowadays Ca–Al and Mg–Al-phosphate minerals have gained recently growing interest in experimental mineralogy because of their stability properties and their potential as index minerals [25]. In this investigation members of the lazulite–scorzalite solid-solution series are synthesized in compositional steps of 12.5 mol% at $T = 485$ °C and $P = 0.3$ GPa under standard hydrothermal conditions and controlled oxygen fugacities of the Ni/NiO-bufer [11]. However, in this work, samples of a lazulite mineral from the Minas Gerais, Brazil has been structurally characterized. Studies include chemistry via electron microprobe analysis in the wavelength dispersive X-ray spectroscopy (WDXS) elemental characterization and structural by means of infrared and Raman, spectroscopic characterization.

Geological setting, occurrence and samples description

The lazulite sample studied in this work was collected from the Gentil mine, a lithium bearing pegmatite located in the municipality of Mendes Pimentel, Minas Gerais, Brazil. The pegmatite is located in the Conselheiro Pena pegmatite district, one of the subdivisions of the Eastern Brazilian Pegmatite province (EBP). The pegmatite district is inserted in the central domain of the Araçuaí mobile belt [26], formed during the Brasiliano orogeny (630–490 Ma) by accretion to the eastern margin of the São Francisco craton. The Gentil pegmatite is mined out and in the past was mined for industrial feldspar and with minor importance of gemstones and samples for the collectors market. The pegmatite is heterogeneous with mineralogical and textural zoning well developed. It has asymmetric lens shape with the longer axis trending to NNE–SSW and body dips about 70° to SSE. The maximum extension is of about 40 m and 12 m thickness. Detailed geology of the pegmatite was described by Chaves [13]. The primary mineral association is represented by quartz, muscovite, microcline, beryl, schorl, almandine–spessartite, triplite and triphylite. The secondary association is mainly composed by albite, Ta and Nb oxides, siderite, elbaite, cassiterite, arsenopyrite, pharmacosiderite and a complex paragenesis of phosphates formed in the result of alteration of triphylite [13,18]. In addition to lazulite, others secondary phosphates, namely autunite, barbosalite, brazilianite, eosphorite, fluorapatite, frondelite, gormanite, heterosite, hureaulite, lithiophillite, matioliite, montebrasite, phosphosiderite, purpurite, roscherite group minerals, scorzalite, souzalite and vivianite are common minerals in miarolitic cavities and in massive blocks formed after the aggregates of primary triphylite up to 0.5 m length [13]. Lazulite nodules up to 3.0 cm long occur in miarolitic cavities, in association with muscovite, triphylite–lithiophilite, gormanite, brazilianite and albite.

Experimental

Samples and preparation

Deep blue and transparent fragments of lazulite were collected from the Gentil mine. The sample was incorporated in the collection of the Geology Department of the Federal University of Ouro Preto, Minas Gerais, Brazil, with sample code SAA-081. The sample is from Gentil mine, a lithium bearing pegmatite with triphylite and spodumene. The mine is located in Mendes Pimentel, east of Minas Gerais. To remove contaminate phases, with the support of a Stereomicroscope Leica Model EZ4, lazulite fragments were handily selected from a sample in association with quartz and muscovite. Lazulite was phase analyzed by X-ray powder diffraction and Scanning electron microscopy in the EDS mode (SEM/EDS). An image of the lazulite sample used in this work is displayed in the Supplementary information and is shown in Fig. S1.

Electron micro probe analysis (EMP)

A quantitative chemical analysis was carried via EMP. Lazulite fragment selected for this study was analyzed with the performance of eight spots. The chemical analysis was carried out with a Jeol JXA8900R spectrometer from the Physics Department of the Federal University of Minas Gerais, Belo Horizonte. For each selected element was used the following standards: Fe–Magnetite, Mn–rodhonite, P and Ca–$Ca_2P_2O_7$, Al–Al_2O_3 and Mg–MgO. The epoxy embedded lazulite sample was polished in the sequence of 9 μm, 6 μm and 1 μm diamond paste MetaDI® II Diamond Paste–Buhler, using water as a lubricant, with a semi-automatic MiniMet® 1000 Grinder–Polisher–Buehler. Finally, the epoxy embedded lazulite was coated with a thin layer of evaporated carbon. The electron probe microanalysis in the WDS (wavelength dispersive spectrometer) mode was obtained at 15 kV accelerating voltage and beam current of 10 nA. Chemical formula was calculated on the basis of ten oxygen atoms (O, OH).

Raman microprobe spectroscopy

Crystals of lazulite were placed on a polished metal surface on the stage of an Olympus BHSM microscope, which is equipped with 10×, 20×, and 50× objectives. The microscope is part of a Renishaw 1000 Raman microscope system, which also includes a monochromator, a filter system and a CCD detector (1024 pixels). The Raman spectra were excited by a Spectra-Physics model 127 He–Ne laser producing highly polarised light at 633 nm and collected at a nominal resolution of 2 cm^{-1} and a precision of ±1 cm^{-1} in the range between 200 and 4000 cm^{-1}. Repeated acquisitions on the crystals using the highest magnification (50×) were accumulated to improve the signal to noise ratio of the spectra. Raman Spectra were calibrated using the 520.5 cm^{-1} line of a silicon wafer. The Raman spectrum of at least 10 crystals was collected to ensure the consistency of the spectra.

A Raman spectrum of lazulite is given in the RRUFF data base (http://rruff.info/Lazulite/R050110). The spectra are given in the Supplementary information. This lazulite mineral sample originated from Rapid Creek, Yukon Territory, Canada. The spectra are shown in Figs. S2–S4. The issue with the spectra as published in

the RRUFF data base is that the spectral range in the OH stretching region is not shown.

Infrared spectroscopy

Infrared spectra were obtained using a Nicolet Nexus 870 FTIR spectrometer with a smart endurance single bounce diamond ATR cell. Spectra over the 4000–525 cm^{-1} range were obtained by the co-addition of 128 scans with a resolution of 4 cm^{-1} and a mirror velocity of 0.6329 cm/s. Spectra were co-added to improve the signal to noise ratio.

Spectral manipulation such as baseline correction/adjustment and smoothing were performed using the Spectracalc software package GRAMS (Galactic Industries Corporation, NH, USA). Band component analysis was undertaken using the Jandel 'Peakfit' software package that enabled the type of fitting function to be selected and allows specific parameters to be fixed or varied accordingly. Band fitting was done using a Lorentzian–Gaussian cross-product function with the minimum number of component bands used for the fitting process. The Gaussian–Lorentzian ratio was maintained at values greater than 0.7 and fitting was undertaken until reproducible results were obtained with squared correlations of r^2 greater than 0.995.

Results and discussion

Chemical characterization

The quantitative chemical analysis of lazulite is presented in Table 1. The composition was calculated as mean values in eight spots. The range of the chemical analysis is also presented, and shows no significant variance. H_2O content was calculated by stoichiometry considering Mg/(Mg + Fe) = 0.89. The chemical formula was calculated on the basis of 10 oxygen atoms (O, OH) in the structure. The chemical composition indicates a magnesium rich phase with partial substitution of magnesium. The results show traces of Ca and Mn, which partially replaces Mg in the tetrahedral site. The chemical formula of the studied sample can be expressed as: $(Mg_{0.88}, Fe_{0.11})Al_{1.87}(PO_4)_{2.08}(OH)_{2.02}$.

Vibrational spectroscopy

In aqueous systems, the Raman spectra of phosphate oxyanions show a symmetric stretching mode (ν_1) at 938 cm^{-1}, an antisymmetric stretching mode (ν_3) at 1017 cm^{-1}, a symmetric bending mode (ν_2) at 420 cm^{-1} and a ν_4 bending mode at 567 cm^{-1} [27–29]. Ross in Farmer (page 404) listed some well-known minerals containing phosphate which were either hydrated or hydroxylated or both [30]. The vibrational spectrum of the dihydrogen phosphate anion has been reported in Farmer. The PO_2 symmetric stretching mode occurs at 1072 cm^{-1} and the POH symmetric stretching mode at ~878 cm^{-1}. The POH antisymmetric stretching mode was at 947 cm^{-1} and the $P(OH)_2$ bending mode at 380 cm^{-1}. The band at 1150 cm^{-1} was assigned to the PO_2 antisymmetric stretching mode. The position of these bands will shift according to the crystal structure of lazulite.

The Raman spectrum of lazulite in the 100–4000 cm^{-1} region is displayed in Fig. 1a. This figure reports the position of the bands and their relative intensity. It is noted that there are regions in the spectrum where no intensity is observed. Therefore, the spectrum is subdivided into sections in subsequent figures so that more detailed assessment of the spectra can be made. In a similar way, the infrared spectrum of matioliite in the 500–4000 cm^{-1} region is reported in Fig. 1b. The spectrum is not shown below 500 cm^{-1}. The reason is that we are using a reflectance technique and the ATR cell absorbs all incident radiation below 500 cm^{-1}. In a similar fashion to the Raman spectrum, the infrared spectrum is divided into sections depending upon the types of vibrations being observed. The Raman spectrum of matioliite in the 800–1400 cm^{-1} region is reported in Fig. 2a. The infrared spectrum of matioliite in the 500–1300 cm^{-1} region is reported in Fig. 2b.

The Raman spectrum is dominated by an intense sharp band at 1060 cm^{-1}. This band is assigned to PO stretching vibrations of HPO_4^{2-} units. The Raman bands at 1019 cm^{-1} is attributed to the PO_4^{3-} stretching vibration. The two Raman bands at 1102 and 1137 cm^{-1} are attributed to both the HOP and PO antisymmetric stretching vibrations. The Raman spectrum of lazulite from the RRUFF data base shown as Figs. S2–S4. A very intense band is observed at 1060 cm^{-1} in harmony with the results of this work. A second intense band in the RRUFF spectrum is found at 1003 cm^{-1} and is attributed to the PO_4^{3-} symmetric stretching vibration. The position of this band shows slight variance from the position of the band reported in this work. Other bands in the RRUFF spectrum are located at 1102, 1137, 1176 and 1219 cm^{-1}. The position and intensity of these bands are in good agreement with the spectrum of this work.

Galy [31] first studied the polarized Raman spectra of the $H_2PO_4^-$ anion. Choi et al. reported the polarization spectra of NaH_2PO_4 crystals. Casciani and Condrate [32] published spectra on brushite and monetite together with synthetic anhydrous monocalcium phosphate ($Ca(H_2PO_4)_2$), monocalcium dihydrogen phosphate hydrate ($Ca(H_2PO_4)_2{\cdot}H_2O$) and octacalcium phosphate ($Ca_8H_2(PO_4)_6{\cdot}5H_2O$). These authors determined band assignments for $Ca(H_2PO_4)$ and reported bands at 1002 and 1011 cm^{-1} as POH and PO stretching vibrations, respectively. The two Raman bands at 1139 and 1165 cm^{-1} are attributed to both the HOP and PO antisymmetric stretching vibrations. Casciani and Condrate [32] tabulated Raman bands at 1132 and 1155 cm^{-1} and assigned these bands to P–O symmetric and the P–O antisymmetric stretching vibrations. Raman spectroscopy identifies the presence of phosphate, hydrogen phosphate and dihydrogen phosphate units in the structure of lazulite.

The infrared spectrum of lazulite (Fig. 2b) shows a complex set of overlapping bands. The two infrared bands at 997 and

Table 1
Chemical composition of lazulite from Gentil pegmatite (mean of 10 electron microprobe analyses). H_2O calculated by stoichiometry.

Constituent	wt.%	Range (wt.%)	Number of atoms	Probe standard/crystal
FeO	1.75	1.48–1.95	0.11	Magnetite/TAP
MgO	11.52	11.20–11.82	0.88	MgO/TAP
Al_2O_3	30.90	30.18–31.71	1.87	Al_2O_3/TAP
P_2O_5	48.30	48.06–48.51	2.08	$Ca_2P_2O_7$/PETJ
MnO	0.01	0.00–0.05	0.00	Rodhonite/LIF
CaO	0.01	0.00–0.02	0.00	$Ca_2P_2O_7$/PETJ
H_2O	5.91	Calculated by stoichiometry	2.02	
Total	98.40		6.94	

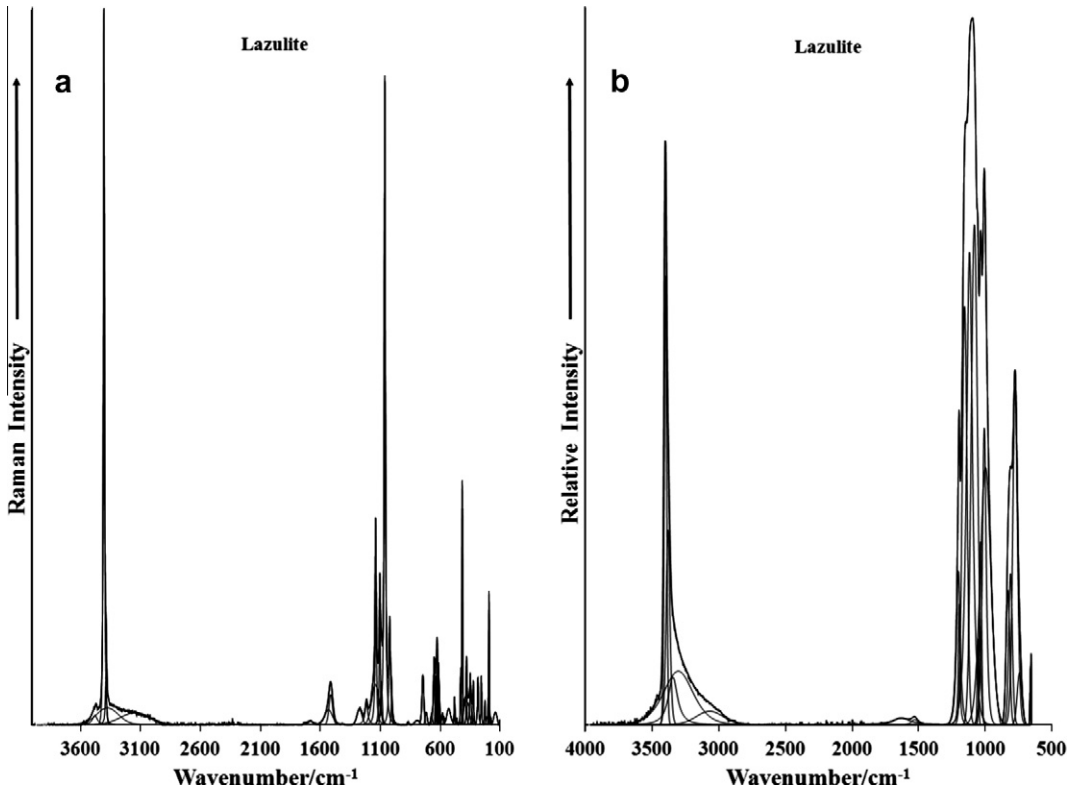

Fig. 1. (a) Raman spectrum of lazulite in the 100–4000 cm^{-1} spectral range, (b) infrared spectrum of lazulite in the 500–4000 cm^{-1} spectral range.

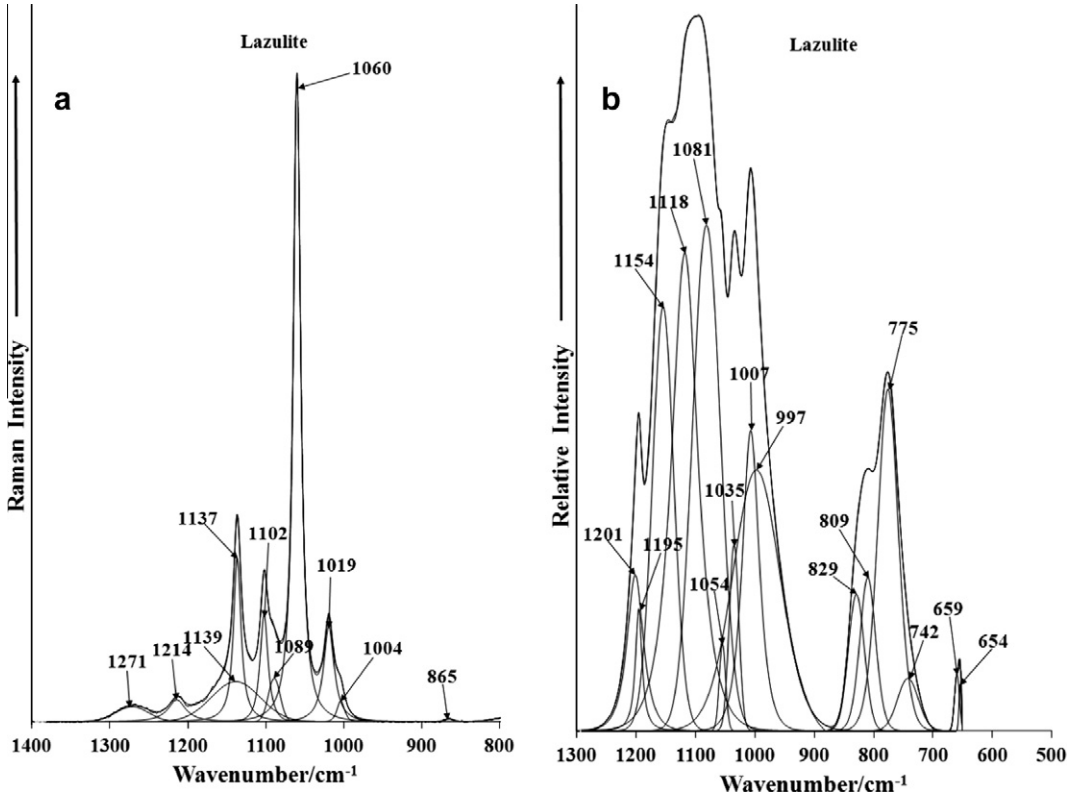

Fig. 2. (a) Raman spectrum of lazulite in the 800–1400 cm^{-1} spectral range, (b) infrared spectrum of lazulite in the 500–1300 cm^{-1} spectral range.

1007 cm^{-1} are attributed to the v_1 PO_4^{3-} symmetric stretching modes. The intense bands at 1035, 1054, 1081, 1118 and 1154 cm^{-1} are assigned to the v_3 PO_4^{3-} antisymmetric stretching modes. The complex set of overlapping infrared bands are attributed to infrared bands due to $H_2PO_4^-$, HPO_4^{2-} and PO_4^{3-} units. If the protons of the hydroxyl units in lazulite are mobile as is likely,

then the protons can be located with the phosphate units thus generating dihydrogen and hydrogen phosphate units.

The Raman spectra of lazulite in the 300–800 cm^{-1} and in the 100–300 cm^{-1} region are shown in Fig. 3a and b respectively. The spectra show the complexity in harmony with the spectrum reported in Fig. 2a and b. The Raman spectral region shown in Fig. 3a represents the bending region of the phosphate units. A set of Raman bands at 605, 613, 633 and 648 cm^{-1} are assigned to the v_4 out of plane bending modes of the PO_4, HPO_4 and H_2PO_4 units. The Raman spectrum of NaH_2PO_4 shows Raman bands at 526, 546 and 618 cm^{-1} (this work). The Raman spectrum of lazulite from the RRUFF data base as shown in Fig. S4. Raman bands are observed in the RRUFF spectrum at 613, 636 and 648 cm^{-1}. The position of these bands is in excellent agreement with the data reported in this work. A very low intensity Raman band is observed at 865 cm^{-1} (Fig. 3a). The assignment of this band is open to question but it is unlikely to be associated with the various phosphate units. One probable assignment is to the deformation modes of the hydroxyl units. The band is also observed in exactly this position in the RRUFF Raman spectrum.

The infrared spectrum (Fig. 2b) is in harmony with the Raman spectrum. Two infrared bands at 654 and 659 cm^{-1} are assigned to this the v_4 out of plane bending modes of the PO_4, HPO_4 units. In the infrared spectrum of dittmarite ($(NH_4)MgPO_4{\cdot}H_2O$) bands are observed at 635 and 656 cm^{-1} and are assigned to the PO_4^{3-} v_4 bending mode. Raman bands are observed at 414, 425, 460 and 479 cm^{-1}. These bands are attributed to the v_2 PO_4, HPO_4 and H_2PO_4 bending modes. The Raman spectrum of NaH_2PO_4 shows Raman bands at 460 and 482 cm^{-1} which are also assigned to this vibrational mode. The Raman spectrum of lazulite downloaded from the RRUFF data base shows bands at 414, 428, 461 and 479 cm^{-1}. The position and intensity of these bands are in harmony with this work.

A set of Raman bands is observed at 322, 347, 365, 378, and 394 cm^{-1}. These bands are considered to be due to metal–oxygen stretching vibrations. Strong Raman bands are observed in the far low wavenumber region at 190, 225, 254 and 282 cm^{-1}. These bands are simply described as lattice vibrations. In the RRUFF spectrum of lazulite, bands are observed at 191, 224, 254 and 283 cm^{-1}. The position of these bands is in great agreement with this work. Some other bands of much lower intensity are observed in the RRUFF Raman spectrum which were not observed in this work.

The Raman spectrum of lazulite and the infrared spectrum in the 2600–3800 cm^{-1} region are illustrated in Fig. 4a and b. The Raman spectrum is dominated by an intense sharp band at 3402 cm^{-1}, assigned to the stretching vibration of the OH units. Other low intensity Raman bands are observed at 3385 and 3478 cm^{-1}. The equivalent infrared band is observed at 3403 cm^{-1}. The band is superimposed upon a spectral profile with additional infrared bands at 3307, 3348 and 3384 cm^{-1}. These bands may be attributed to water stretching vibrations. The Raman spectrum of lazulite in the 1400–1800 cm^{-1} and the infrared spectrum in the 1300–1800 cm^{-1} are reported in Fig. 5a and b respectively. These spectra are quite noisy; nevertheless a low intensity Raman band is found at 1684 cm^{-1} with two additional bands at 1509 and 1528 cm^{-1}. The first band is assigned to strongly bonded water molecules. The latter two bands are thought to be overtone or combination bands. In the infrared spectrum, two bands are observed at 1530 and 1630 cm^{-1}.

Conclusions

The minerals of lazulite group are basic hydroxy-phosphates and arsenates with the general chemical composition $M_1^{2+}M)_2^{3+}(XO_4)_2(OH)_2$, where M_1 can be occupied by Fe^{2+}, Mg, Cu and Zn, and M_2 can be occupied by Al and Fe^{3+}. In the anionic group, X can be occupied by P and As. The minerals crystallize in the monoclinic crystal system, space group $P2_1/c$. In this work we have studied a lazulite collected from the Gentil mine, a lithium bearing

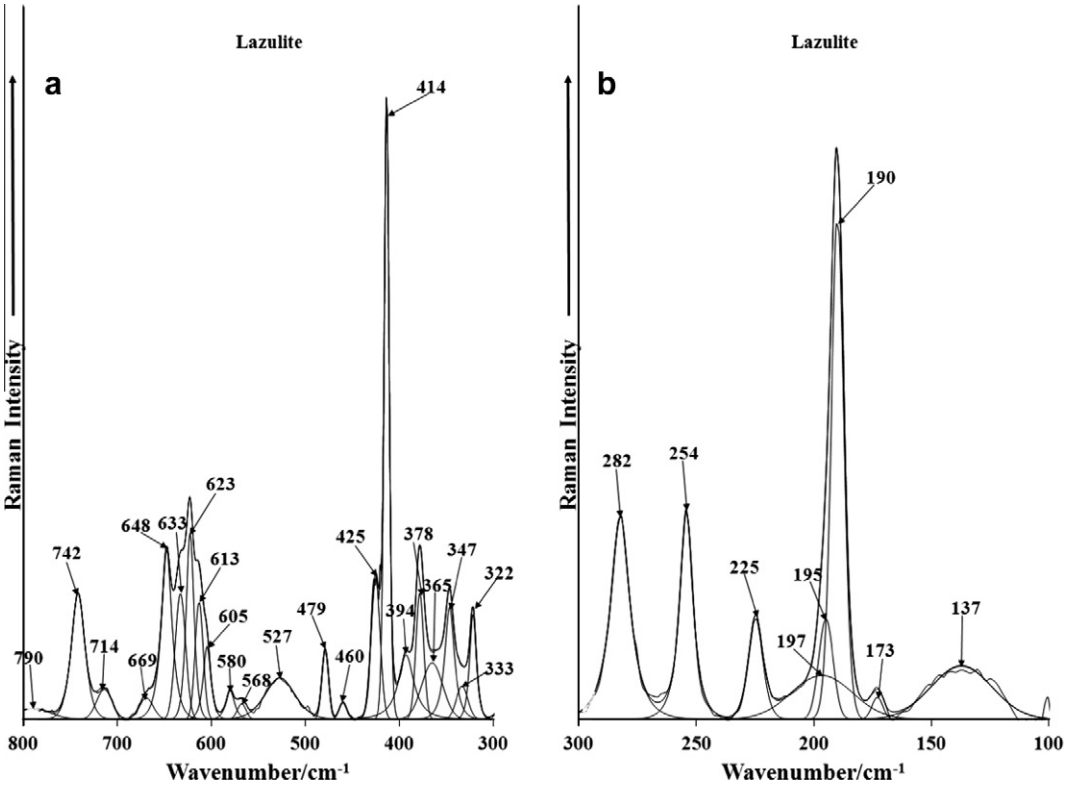

Fig. 3. (a) Raman spectrum of lazulite in the 300–800 cm^{-1} spectral range, (b) Raman spectrum of lazulite in the 100–300 cm^{-1} spectral range.

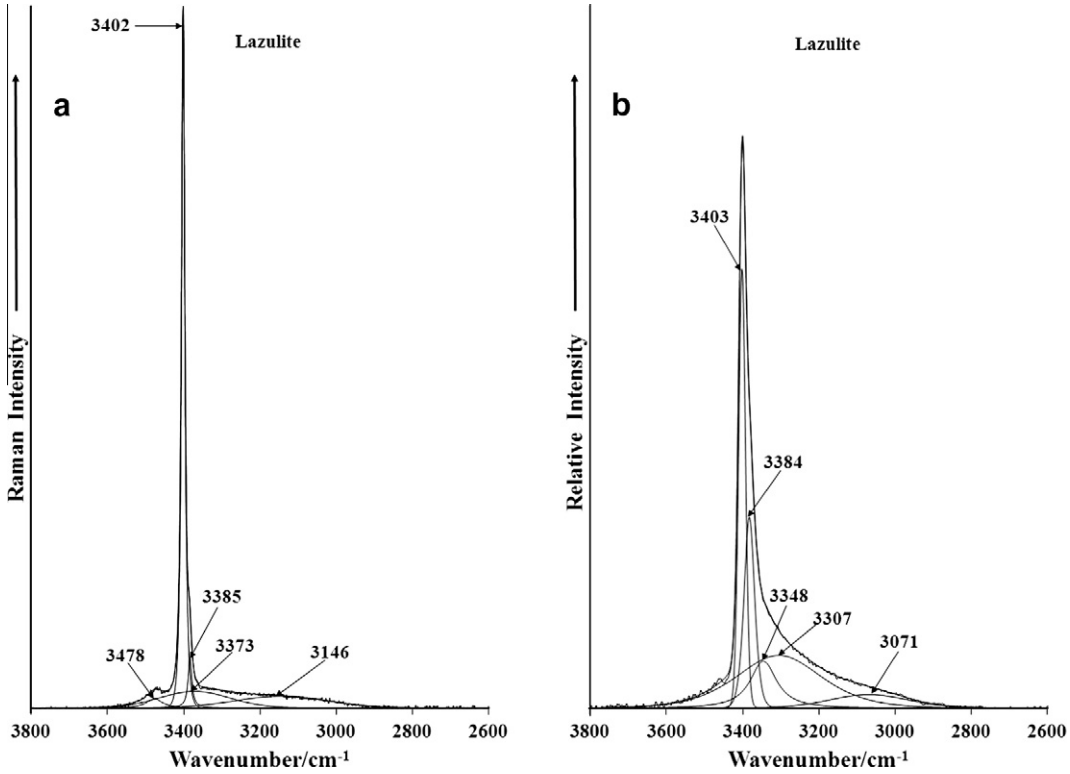

Fig. 4. (a) Raman spectrum of lazulite in the 2600–3800 cm^{-1} spectral range, (b) infrared spectrum of lazulite in the 2600–3800 cm^{-1} spectral range.

pegmatite located in the municipality of Mendes Pimentel, Minas Gerais, Brazil. The pegmatite is located in the Conselheiro Pena pegmatite district, one of the subdivisions of the Eastern Brazilian Pegmatite province (EBP). Chemical analysis of the mineral was undertaken using EDX techniques and the formula of the mineral was found to be $(Mg_{0.88}, Fe_{0.11})Al_{1.87}(PO_4)_{2.08}(OH)_{2.02}$. Aspects of the structure of lazulite using vibrational spectroscopy were assessed. Raman and infrared bands associated with dihydrogen

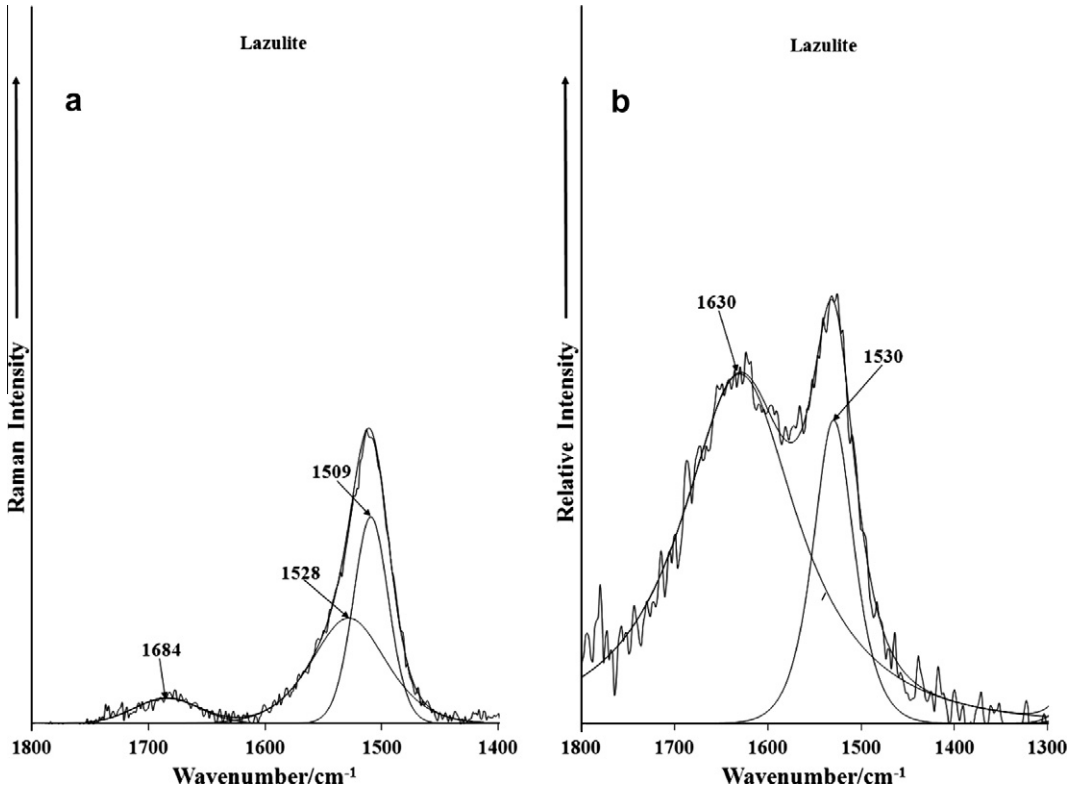

Fig. 5. (a) Raman spectrum of lazulite in the 1400–1800 cm^{-1} spectral range, (b) infrared spectrum of lazulite in the 1300–1800 cm^{-1} spectral range.

phosphate, hydrogen phosphate and phosphate units were observed. It is apparent that all three anion types exist in the structure of lazulite and these anionic types are enhanced by the basic nature of the mineral. The proton on the hydroxyl units is apparently very mobile and enables the formation of the monohydrogen and dihydrogen phosphate units. Only a single very intense band at around 3402 cm^{-1} in both the Raman and infrared spectra is assigned to the stretching of the OH units in the lazulite structure. Vibrational spectroscopy enabled an assessment of the molecular structure of lazulite to be made.

Acknowledgements

The financial and infra-structure support of the Discipline of Nanotechnology and Molecular Science, Science and Engineering Faculty of the Queensland University of Technology, is gratefully acknowledged. The Australian Research Council (ARC) is thanked for funding the instrumentation. R. Scholz thanks to FAPEMIG – Fundação de Amparo à Pesquisa do Estado de Minas Gerais (Grant No. CRA – APQ-03998-10). Martina Beganovic is grateful to CNPq for the master's scholarship.

Appendix A. Supplementary material

Supplementary data associated with this article can be found, in the online version, at http://dx.doi.org/10.1016/j.saa.2013.01.056.

References

[1] M.E. Back, J.A. Mandarino, Fleischer's glossary of mineral species, Mineral. Rec. (2008) 343.
[2] M.L. Lindberg, W.T. Pecora, Am. Mineral. 40 (1955) 952–966.
[3] S.A. Abernathy, F.N. Blanchard, Am. Mineral. 67 (1982) 610–614.
[4] M.H. Klaproth, Beiträge zur chemischen Kenntniss der Mineralkörper, 1795.
[5] N.H.W. Sieber, E. Tillmanns, O. Medenbach, Am. Mineral. 72 (1987) 404–408.
[6] M.B. Duggan, M.T. Jones, D.N.G. Richards, J.L. Kamprad, Can. Mineral. 28 (1990) 125–131.
[7] P. Schmid-Beurmann, S. Knitter, L. Cemic, Mineral. Petrol. 70 (2000) 55–71.
[8] P.B. Moore, Am. Mineral. 55 (1970) 135–169.
[9] R. Selke, P. Schmid-Beurmann, L. Cemic, Euro. J. Mineral. 15 (2003) 127–136.
[10] G. Morteani, D. Ackermand, Mineral. Petrol. 80 (2004) 59–81.
[11] P. Schmid-Beurmann, S. Knitter, L. Cemic, Phys. Chem. Mineral. 26 (1999) 496–505.
[12] G. Morteani, D. Ackermand, Neues Jahrb. Mineral. 182 (2006) 123–148.
[13] M.L.S.C. Chaves, Aust. Gem. 21 (2003) 390–399.
[14] D. Ackermand, G. Morteani, T. Razakamanana, Proc. German-Malagasy Res. Cooperation in Life and Earth Sciences, 2006, pp. 5–18.
[15] I.A. Izbrodin, G.S. Ripp, N.S. Karmanov, Geol. Ore Dep. 51 (2009) 617–626.
[16] P. Uher, T. Mikus, R. Milovsky, A. Biron, J. Spisiak, J. Lipka, J. Jahn, Lithos 112 (2009) 447–460.
[17] G.W. Robinson, J.v. Velthuizen, H.G. Ansell, B.D. Sturman, Mineral. Rec. 23 (1992) 1–47.
[18] D. Atencio, J.M.V. Coutinho, M.Y.P.J. Ellena, Am. Mineral. 91 (2006) 1932–1936.
[19] H.G. Dill, F. Melcher, A. Gerdes, B. Weber, Can. Mineral. 46 (2008) 1131–1157.
[20] S. Bajanik, Mineral. Slov. 11 (1979) 473–476.
[21] M.-Y. Chen, Xueyuan Xuebao (1979) 126–127.
[22] D.N. Litoshko, V.V. Bukanov, Zapiski Vses. Min. Obsh. 118 (1989) 35–41.
[23] R. Simeone, Rivista Min. Ital. (1980) 52–56.
[24] Y. Yang, Y. Guo, J. Liu, Y. Zhang, Y. Li, N. Chou, C. Chen, Zhongguo Dizhi Kexueyuan Kuangchuang Dizhi Yanjiuso Sokan 15 (1985) 149–156.
[25] L. Cemic, P. Schmid-Beurmann, Euro. J. Mineral. 7 (1995) 921–929.
[26] F.F.M. Almeida, O. Craton do São Francisco, Revista Brasileira de Geociências (in Portuguese) 7 (1977) 349–364.
[27] R.L. Frost, W. Martens, P.A. Williams, J.T. Kloprogge, Mineral. Mag. 66 (2002) 1063–1073.
[28] R.L. Frost, W.N. Martens, T. Kloprogge, P.A. Williams, Neues Jahrb. Mineral. (2002) 481–496.
[29] R.L. Frost, P.A. Williams, W. Martens, J.T. Kloprogge, P. Leverett, J. Raman Spectrosc. 33 (2002) 260–263.
[30] V.C. Farmer, Mineralogical Society Monograph 4: The Infrared Spectra of Minerals, The Mineralogical Society, London, 1974.
[31] A. Galy, J. Phys. Rad. 12 (1951) 827.
[32] F.S. Casciani, R.A. Condrate, Sr., in: Proceedings – International Congress on Phosphorus Compounds, second ed., 1980, pp. 175–190.